Advances in Science and Technology Research Journal
Volume 8, No. 23, Sept. 2014, pages 62–67
DOI: 10.12913/22998624.1120324

Research Article

BROADBAND CONCEPT OF ENERGY HARVESTING IN BEAM VIBRATING SYSTEMS FOR POWERING SENSORS

Andrzej Rysak[1], Michael Müller[2], Marek Borowiec[1], Jarosław Zubrzycki[1], Grzegorz Litak[1], Anna Godlewska-Lach[1], Volker Wittstock[2]

[1] Faculty of Mechanical Engineering, Lublin University of Technology, 20-618 Lublin, Poland; e-mail: a.rysak@pollub.pl; m.borowiec@pollub.pl; j.zubrzycki@pollub.pl; g.litak@pollub.pl; anna.godlewska@pollub.eu.pl

[2] Technische Universität Chemnitz, Institut für Werkzeugmaschinen und Produktionsprozesse Reichenhainer, 09126 Chemnitz, Germany, e-mail: michael.mueller@mb.tu-chemnitz.de; volker.wittstock@mb.tu-chemnitz.de

Received: 2014.08.02
Accepted: 2014.08.18
Published: 2014.09.09

ABSTRACT
Recent demand for powering small sensors for wireless health monitoring triggered activities in the field of small size efficient energy harvesting devices. We examine energy harvesting in an aluminium beam with a piezoceramic patch subjected to kinematic harmonic excitation and impacts. Due to a mechanical stopper applied, inducing a hardening effect in the spring characteristic of the beam resonator, we observed a broader frequency range for the fairly large power output. Impact nonlinearities caused sensitivity to initial conditions and appearance of multiple solutions. The occurrence of resonant solution associated with impacts increased efficiency of the energy harvesting process.

Keywords: piezoceramic, energy harvesting, vibration, broadband effect, impacts.

INTRODUCTION

The existence of non-linearities in mechanical systems usually shows complex dynamical responses by a non-trivial dependence of amplitude and frequency, vibration localization, and also by occurrence of multiple solution. These nonlinear effects can improve the effectiveness of energy harvesting systems in capturing the vibration kinetic energy, through the so called broadband frequency effect [1–7]. Corresponding devices of energy harvesting contain mechanical resonators and additional energy transducers for transforming ambient mechanical energy into the electric form. This direction of reseach was continued by Blystad and Halvorsen [8]. On the other hand, the papers [9–11] studied extensively micro-electromechanical systems proposing applications of the electrostatic devices for energy harvesting. Additionally, Gu and Livermore [9] presented experimental results of models of energy harvesting devices in which a low frequency resonator impacts a high frequency harvesting resonator. Such experiments prove that the efficiency of the electrical power transfers can be significantly improved. The paper continues studies on non-linear impacting piezocaramic harvesters with stoppers, drawing attention to broadening the energy harvesting efficiency characteristic demonstrated by authors of Gu and Livermore [9] and Soliman et al. [12,13] and Borowiec et al. [14]. Finally, Rysak et al. [15] performed modal analysis of the broadband vertical beam energy harvester with the moving mass including additional impacts and friction phenomena. In the analyzed real experimental model, the influence of an applied mechanical stopper on the efficiency of the piezoceramic layers in the vibrating structure is investigated. Note that the impacts of the cantilever into the stopper not only limit vertical displacements but do also change the spring characteristics of the vibrating beam which increases the resonant resonant frequency.

PZT material included in the piezoelectric, initially polarized fibres was prepared in Chemnitz TU and is characterized by a unique electrical

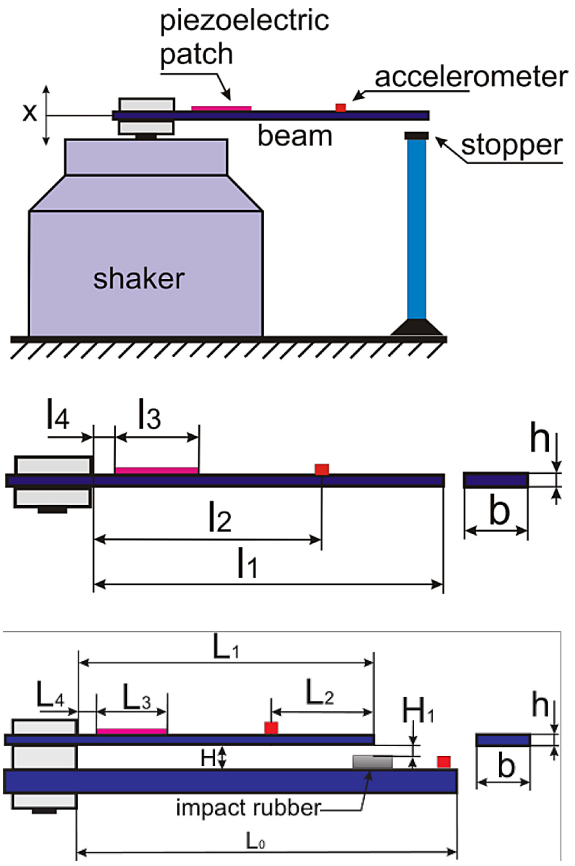

Fig. 1. Experimental stand (a), note the location of the piezoceramic patch, and accelerometer (sensor). Characteristic dimensions of the excited aluminum beam (b), and the two impacting beam system (c). To minimize the risk of fracture of the piezoceramic element we placed the thin layer of rubber on the stopper in both configurations (see Fig. a-b and c). The system geometrical and material parameters are included in Table 1. The lower beam is Fig. 1c is much more rigid having the resonance frequency fairly outside the examined region

impedance. Figure 3 shows the measured impedance amplitude and related angle provided by the HIOKI 3532-50 impedance meter. Impedance is inversely proportional to frequency and the angle changes are due to the influence of small ohmic resistivity caused by electrical lead connections.

EXPERIMENTAL MODEL

The measurements have been performed on a vibration generator TIRAvib TV 50101, which operated in a sine mode under controlled conditions. The schematic setup is presented in Fig. 1a. The beam with attached piezoceramic layers was excited in vertical direction in the vicinity of the principal resonance. The piezoceramic patch consisted of ten piezoceramic fibres (PZT) uti-

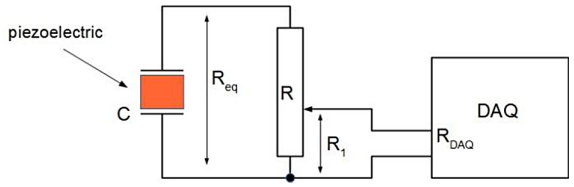

Fig. 2. Electrical circuit set with the electro-motive force on the piezoceramic element; the circuit of the voltage divider was used in order to adjust the measured voltage to the range available for the DAQ card

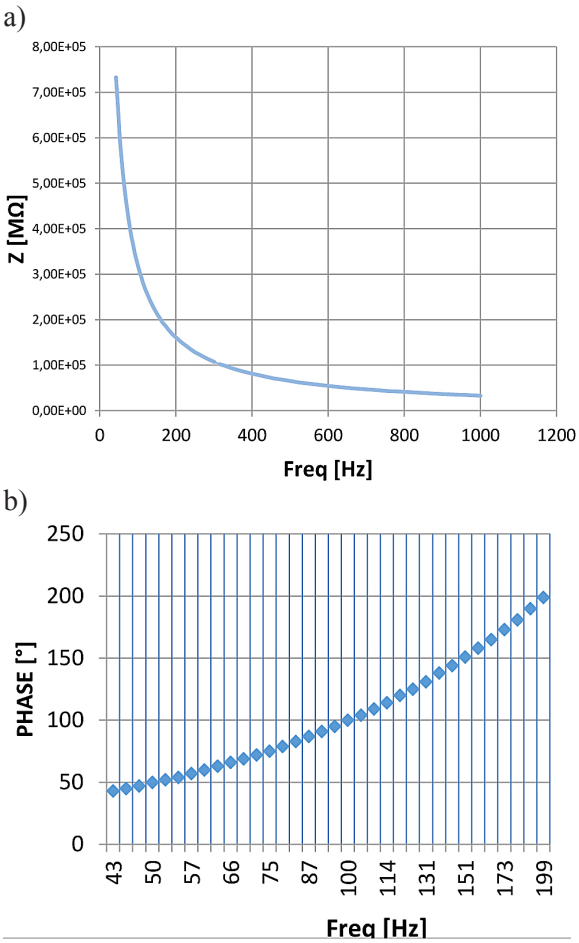

Fig. 3. Frequency dependence of the impedance (3a), frequency dependence of the angle θ (3b); Research on the meter Hioki 3532-50

lizing d_{31}-effect. The fibers (PZT) were bounded with Elecolit isotropic conductive adhesive and insulated by globe top (epoxy resin). We worked in two configurations; with the fixed (Figs. 1a-b) and moving frame (Fig. 1c) stoppers.

During the beam vibration, the electric power output is generated by the piezoelectric elements while the electrical circuit is loaded by corresponding resistors (Fig. 2). The electrical output was measured by means of data acquisition set (DAQ) (see Fig. 2) as:

$$U_{DAQ} = U_{out}\frac{R_1}{R} \quad (1)$$

where: R_1/R is the voltage divider presented in Figure 2, applied to avoid exceeding the measurement voltage range. In the experiments we used piezoceramic fibre patch.

Note that the two discussed configurations (Figs. 1 a-b and c) differ in the excitation the first of them (Figs. 1a-b) is characterized in additional parametric excitation as the effective distance between the beam and stopper is modulated with the excitation frequency:

$$h_1' = h_1 - \frac{A}{\omega^2}\sin(\omega t) \quad (2)$$

On the other hand, in the second case (Fig. 1c), the distance H^1 is fixed.

ANALYSIS OF EXPERIMENTAL RESULTS

The measurements have been done using two different distances between the fixed and moving stoppers and vibrating beam (Fig. 1). The results for two sets are shown in Figures 3a and b, by means of resonance curves of gravitation force captured by the accelerometer mounted on the beam. Figure 4a presents behaviour in case of stopper gap (measured for a motionless beam) being 6.5 mm, and in Figure 4b gap being 11 mm. Finally, Figure 3c represents the double beams with the distance between them of 14.3 mm.

Firstly, it is easy to notice the difference for increasing gap (see Figs. 4a and b), when the stopper is less engaged. Moreover, vibrating the beam with impacts leads to increasing the energy harvesting efficiency through the resonant solution appearing for higher frequencies. Such behaviour manifests in hardening the beam stiffness characteristic and next broadening the reached level of the measured amplitude. The beam was subjected to kinematic periodic excitation with the increasing and decreasing frequency sweeps (in Figs. 4a, b, blue and red lines respectively). On the right hand side of the resonance centre we observe at least two solutions indicating resonant (impacting) and non-resonant solutions due to the stopper induced hardening of the effective beam stiffness. Interestingly, the two solutions (see blue and red lines) are also observed on the left hand side of the resonance center. This looks like stiffness softening originating in the contact between the beam and stopper. Note that this contact was realized through a thin layer of rubber.

The broadening in the non-resonant solution branch is presumably caused by air circulations between macroscopic beam and stopper. Note that it decreases with the growing distance between the beam and stopper. Secondly, to clarify

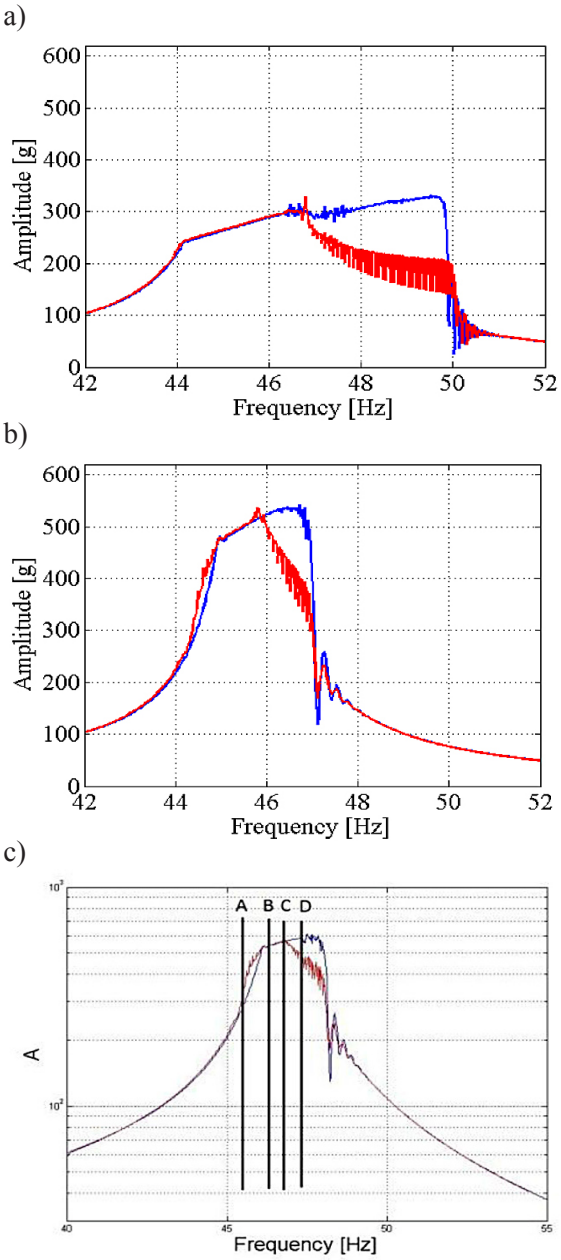

Fig. 4. Amplitude of inertial acceleration output versus frequency at different gap sizes between beam and independent stopper: h^1 =6.5 mm (a) and 11 mm (b). Figure (c) presents the same dependency of the amplitude A as a function of frequency for the system of double beams with the distance between beams equals to H_1 =14.3 mm. The blue and red lines correspond to up and down frequency sweep, respectively. Note that we limited the discussion to the first mode shape of beam vibration

Table 1. Parameters of the mechanical resonator and electrical circuit

Symbol and value	Description
b = 20 mm	beam width
h = 1.5 mm	beam thickness
h^1 , h_1'	distances between the beam and stopper for the stationary and moving set, respectively (Fig. 1a)
$L_1 = l_1$ = 163 mm	beam length
l_2 = 98 mm, L_2 = 65 mm	positions of the accelerometer
$L_3 = l_3$ = 20 mm	length of the piezoceramic layer
$L_4 = l_4$ = 12 mm	position of the piezoceramic layer
H_1 = 14.3 mm	distance between beams in double beam system
R_{DAQ} = 127 kΩ	internal impedance of DAQ
R_{eq} = 30.5 kΩ	equivalent load for the attached circuit
E = 69 GPa	Young modulus of the beam
ρ = 2.7 g/cm^3	density the beam material
A = 2 g	acceleration amplitude
C = 4.9 nF	capacity of the piezoceramic layer
11.5 mm × 0.24 mm	dimensions of the piezoceramic
× 0.26 mm	fibers (PZT)
N = 10	number of parallel fibres in the piezoceramic layer
ω	excitation frequency

the dynamical response (of Figs. 4a-b cases) we present Figure 5 reflecting the evolution of the voltage time series along the resonance curve for the gap between the beam and stopper of 11 mm (Fig. 4b). The characteristic impact influences are noticeable in Figures 4b and c. On the other hand, Figures 4d-f correspond to non-resonant solutions. Finally, in Fig. 6 we show the corresponding time series for the last case (of Fig. 4c). Here the impacts are also clearly visible in the contact regions = 46.46 Hz (b) and 46.82 Hz (c), while the outer cases Figure 6a and 6d indicate the motion without impacts.

CONCLUSIONS

We studied the effect of stopper on vibration energy scavenging in two configurations (fixed and moving frame stoppers). Decreasing the distance between stopper and mechanical beam resonator introduced hardening to the system stiffness. Consequently, it also influenced the process of energy harvesting significantly, leading to increasing the frequency range and finally

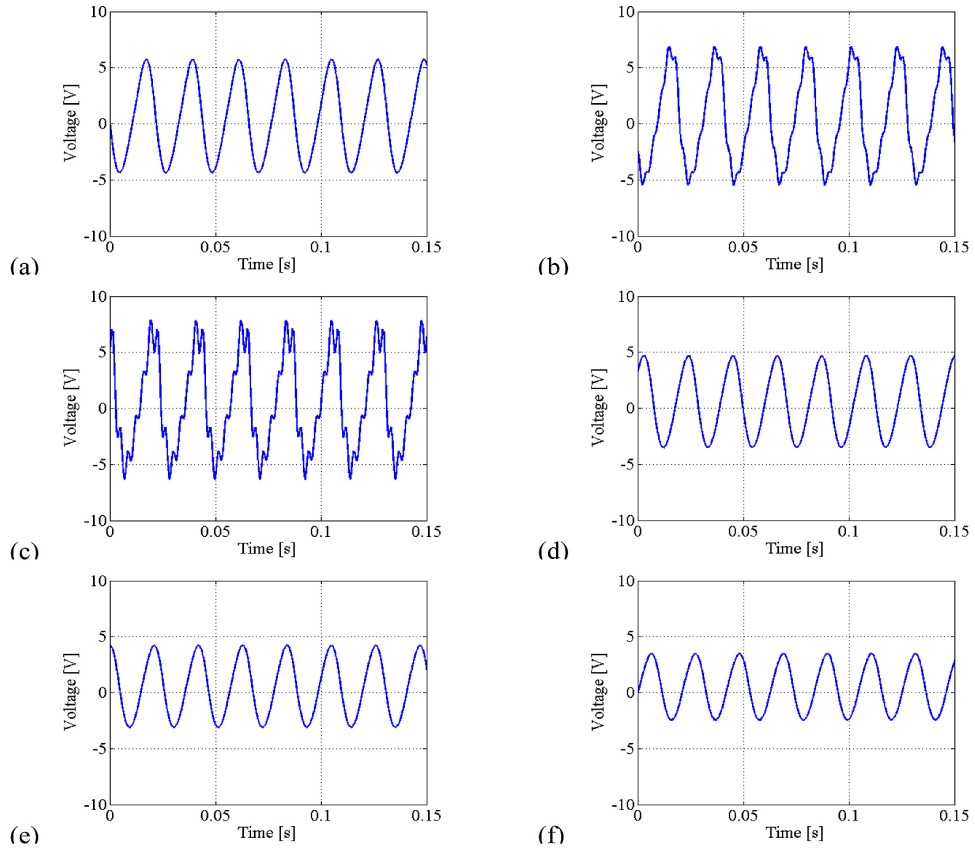

Fig. 5. Time series of voltage output measured at the gap size 11mm (case presented in Fig. 3 b). The excitation frequencies for consecutive time series were: (a) f_{exc} = 44.70 Hz, (b) f_{exc} = 45.40 Hz, (c) f_{exc} = 45.86 Hz, (d) f_{exc} = 46.56 Hz, (e) f_{exc} = 46.72 Hz, (f) f_{exc} = 47.06 Hz respectively. The voltage variance (in V^2 units) proportional to the power output for the consecutive cases are following: 12.32 (a), 16.5 (b), 18.33 (c), 8.2 (d), 6.61 (e), and 4.36 (f)

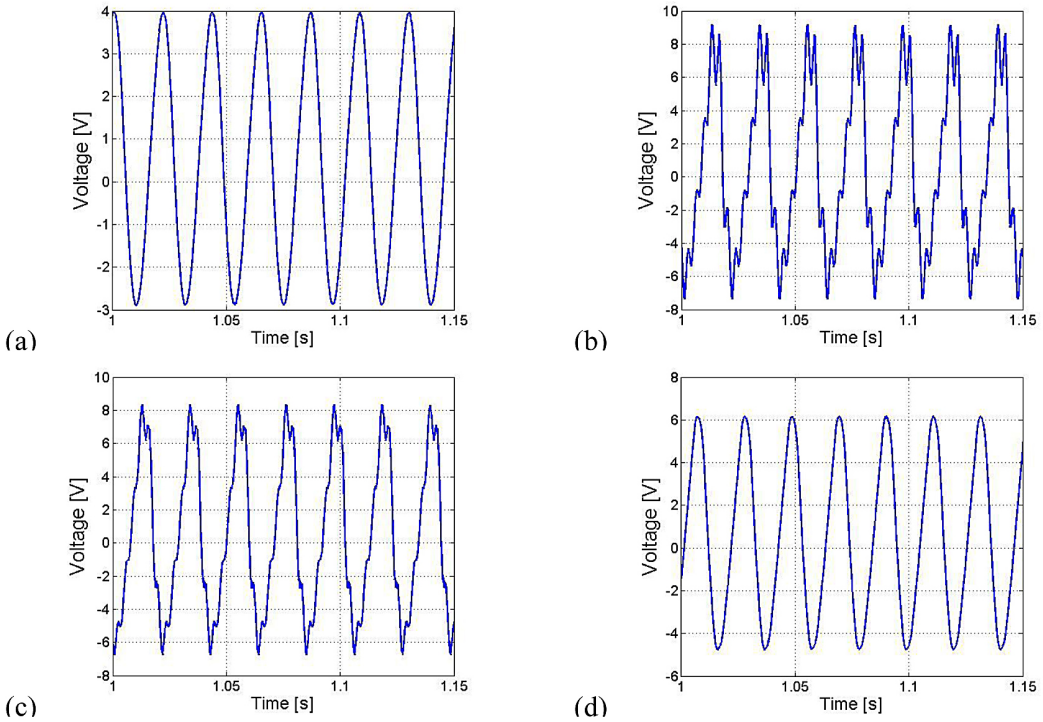

Fig. 6. Time series of voltage output measured at the gap size 14.3 mm (case presented in Fig. 3 c). The excitation frequencies for consecutive time series were: (a) f_{exc} = 45.40Hz, (b) f_{exc} = 46.46 Hz, (c) f_{exc} = 46.82 Hz, (d) f_{exc} = 47.32 Hz, respectively. Values of frequencies were marked on Figure 3c with subsequent names: A, B, C, and D The voltage variance (in V^2 units) proportional to the power output for the consecutive cases are following: 5.81 (a), 22.23 (b), 24.13 (c), 14.60 (d)

to the broadband effect. The evolution of the acceleration and voltage outputs measured along the amplitude-frequency diagram confirms the increase of the vibration amplitude, and consequently, the improvement of the power output in the frequency broad band form. In that region of frequency we noticed multiple solutions by doing up and down frequency sweeps. Obviously the improvement energy harvesting is associated with increasing range of impacting solution. It is worth to notice that in cases of the resonant (impacting) and non-resonant (non-impacting) solutions the percentage of the corresponding basins of attraction area are changing with the frequency. According to the findings of Borowiec et al. [14] where the ratio is changing from 1 to 0 for growing frequency.

Acknowledgments

This research was supported by the Polish National Science Center (A.R., M.B., J.Z., and G.L.) under the grant agreement No. 2012/05/B/ST8/00080 and by the Deutsche Forschungsgemeinschaft (DFG) in context of the Collaborative Research Centre/Transregio 39 PT-PIESA (M.M. and V.W.), subproject A2.

REFERENCES

1. Beeby S.P., Tudor M.J., White N.M., Energy harvesting vibration sources for microsystems applications. Measurement Science and Technology 17, 2006, 175–195.
2. Mitcheson P.D., Yeatman E.M., Rao G.K., Holmes A.S., Green T.C., Energy harvesting from human and machine motion for wireless electronic devices. Proc. IEEE 96, 2008, 1457–1486.
3. Erturk A., Inman D., Piezoelectric Energy Harvesting. Chichester: John Wiley & Sons Ltd. 2011.
4. Harne R.L., Wang K.W., A review of the recent research on vibration energy harvesting via bistable systems, Smart Mater. Struct. 22, 2012, 023001.
5. Friswell M.I., Ali S.F., Adhikari S., Lees A.W., Bilgen O., Litak G., Nonlinear piezoelectric vibration energy harvesting from a vertical cantilever beam with tip mass J. Intellig. Mat. Syst. Struct. 23, 2012, 1505–1521.
6. Litak G., Friswell M.I., Kwuimy C.A.K., Adhikari S., Borowiec M., Energy harvesting by two magnetopiezoelastic oscillators with mistuning, Theoret. Appl. Mech. Lett. 2, 2012, 043009.
7. Kwuimy C.A.K., Litak G., Borowiec M., Nataraj C., Performance of a piezoelectric energy harvester dri-ven by air flow, Appl. Phys. Lett. 100, 2012, 024103.

8. Blystad L-C. J., Halvorsen E., A piezoelectric energy harvester with a mechanical end stop on one side, Microsyst. Technol. 17, 2011, 505–511.
9. Gu L., Livermore C., Impact-driven, frequency up-converting coupled vibration energy harvesting device for low frequency operation Smart Mater. Struct. 20, 2011, 045004.
10. Le C.P., Halvorsen E., Sorasen O., Yeatman E.M., Microscale electrostatic energy harvester using internal impacts J. Intellig. Mat. Syst. Struct. 23, 2012, 1409–1421.
11. Le C.P., Halvorsen E., MEMS electrostatic energy harvesters with end-stop effects, J. Micromech. Microeng. 22, 2012, 074006.
12. Soliman M.S.M., Abdel-Rahman E.M., El-Saadany E.F., Mansour R.R., A wideband vibration-based energy harvester, J. Micromech. Microeng. 18, 2008, 115021.
13. Soliman M.S.M., Abdel-Rahman E.M., El-Saadany E.F., Mansour R.R., Design procedure for wideband micropower generators, J. Mircoelectromech. Systems 18, 2009, 1288–1299.
14. Borowiec M., Litak G., Lenci S., Basins of attraction in a simple harvesting system with a stopper. In: J.T.A Machado, D. Baleanu, A. Luo (Eds.), Discontinuity and Complexity in Nonlinear Physical System, Vol. 6, 315, 2014, 315–321.
15. Rysak A., Scheffler M., Gier J., Borowiec M., Litak G., Broadband vertical beam energy harvester with the moving mass. Latin American Journal of Solids and Structures, submitted 2013.